

Verification of antiferromagnetic exchange coupling at room temperature using polar magneto-optic Kerr effect in thin EuS/Co multilayers with perpendicular magnetic anisotropy

A. Goschew, M. Scott, and P. Fumagalli

Citation: *Applied Physics Letters* **109**, 062401 (2016); doi: 10.1063/1.4960794

View online: <http://dx.doi.org/10.1063/1.4960794>

View Table of Contents: <http://scitation.aip.org/content/aip/journal/apl/109/6?ver=pdfcov>

Published by the [AIP Publishing](#)

Articles you may be interested in

[Variable angle magnetometry for exchange-coupled multilayers with in-plane and perpendicular anisotropy](#)
J. Appl. Phys. **110**, 123905 (2011); 10.1063/1.3665191

[Ferrimagnetic stripe domain formation in antiferromagnetically-coupled Co/Pt–Co/Ni–Co/Pt multilayers studied via soft x-ray techniques](#)
Appl. Phys. Lett. **98**, 172503 (2011); 10.1063/1.3583454

[Using exchange bias to extend the temperature range of square loop behavior in \[Pt/Co \] multilayers with perpendicular anisotropy](#)
Appl. Phys. Lett. **87**, 242504 (2005); 10.1063/1.2139840

[Correlation between perpendicular exchange bias and magnetic anisotropy in IrMn/\[Co/Pt \]_n and \[Pt/Co \]_n/IrMn multilayers](#)
J. Appl. Phys. **97**, 063907 (2005); 10.1063/1.1861964

[Exchange-biased spin valves with perpendicular magnetic anisotropy based on \(Co/Pt\) multilayers](#)
J. Appl. Phys. **93**, 8397 (2003); 10.1063/1.1558096

The advertisement features a Lake Shore Model 372 cryogenic temperature controller on the left. The device is a white, rectangular unit with a digital display showing '96.837' and several control buttons. To the right of the device is a detailed, close-up photograph of a cryogenic system, showing various metal components, pipes, and a large cylindrical vessel, all set against a blue background. The text 'Precise temperature control for cryogenic research' is written in white on the left side of the image. The Lake Shore CRYOTRONICS logo is in the top right corner.

Precise temperature control
for cryogenic research

Model 372

Lake Shore
CRYOTRONICS

Verification of antiferromagnetic exchange coupling at room temperature using polar magneto-optic Kerr effect in thin EuS/Co multilayers with perpendicular magnetic anisotropy

A. Goschew,^{a)} M. Scott, and P. Fumagalli

Institut für Experimentalphysik, Freie Universität Berlin, Arnimallee 14, 14195 Berlin, Germany

(Received 21 April 2016; accepted 30 July 2016; published online 9 August 2016)

We report on magneto-optic Kerr measurements in polar geometry carried out on a series of thin Co/EuS multilayers on suitable Co/Pd-multilayer substrates. Thin Co/EuS multilayers of a few nanometers individual layer thickness usually have their magnetization in plane. Co/Pd multilayers introduce a perpendicular magnetic anisotropy in the Co/EuS layers deposited on top, thus making it possible to measure magneto-optic signals in the polar geometry in remanence in order to study exchange coupling. Magneto-optic Kerr-effect spectra and hysteresis loops were recorded in the visible and ultraviolet photon-energy range at room temperature. The EuS contribution to the magneto-optic signal is extracted at 4.1 eV by combining hysteresis loops measured at different photon energies with polar magneto-optic Kerr-effect spectra recorded in remanence and in an applied magnetic field of 2.2 T. The extracted EuS signal shows clear signs of antiferromagnetic coupling of the Eu magnetic moments to the Co layers. This implies that the ordering temperature of at least a fraction of the EuS layers is above room temperature proving that magneto-optic Kerr-effect spectroscopy can be used here as a quasi-element-specific method. © 2016 Author(s). All article content, except where otherwise noted, is licensed under a Creative Commons Attribution (CC BY) license (<http://creativecommons.org/licenses/by/4.0/>). [<http://dx.doi.org/10.1063/1.4960794>]

Since the discovery of ferromagnetism in the semiconductor ($E_g = 1.65$ eV) Europium sulfide (EuS) in 1962,¹ it has been the target of many investigations and theoretical calculations. Ferromagnetism in EuS is purely spin-related as it originates in the highly localized, half-filled $4f$ shell, leading to a spectroscopic ground state $^8S_{7/2}$ and making EuS an ideal Heisenberg ferromagnet.

EuS is a promising candidate for the realization of a spin polarized current within a semiconductor. However, its low Curie temperature of only 16.5 K is a major drawback. While a lot of effort has been put into increasing the ordering temperature,^{2,3} the Curie temperature could not be raised to room temperature (RT) until recently. A new approach including the use of multilayers of EuS and ferromagnetic $3d$ transition metals, such as Co and Ni, has shown promising results with clear evidence of spin polarization in EuS at room temperature.^{4,5} Antiferromagnetic coupling is known to exist in $3d-4f$ alloys^{6,7} and has been observed in the case of Fe⁸ and Co^{9,10} at low temperatures where EuS is ferromagnetic. As was shown by X-ray magnetic circular dichroism (XMCD) measurements on Co/EuS multilayers, the antiferromagnetic coupling between Co and EuS could not be fully broken up at 5 K. The EuS XMCD signal at room temperature for the same multilayers was considerably weaker than that at low temperatures but nevertheless still present. This suggests that the antiferromagnetic coupling between Co and EuS is still present at RT, however, somewhat weaker.

The main aim of this work is to find evidence of antiferromagnetic coupling between Co and EuS at RT and possibly coupling breaking, by measuring the magneto-optic Kerr effect (MOKE) in polar geometry. MOKE is a simple technique and

highly sensitive down to a few monolayers, but it does not measure *per se* element specifically. However, in inhomogeneous systems, such as the multilayers investigated here, taking advantage of spectral information enables under certain conditions quasi-element-specific measurements.^{3,11} In order to extract the EuS signal from the Co/EuS multilayers, we make simple yet justified assumptions, based on earlier XMCD measurements of similar multilayer systems.

All samples were prepared by e-beam evaporation in ultra-high vacuum (UHV) in a Balzers UMS 630 chamber with base pressure of around 1×10^{-8} mbar. Electron-beam evaporation is the technique best suited for EuS evaporation because of the high sublimation temperature (~ 2400 °C) of EuS. Powder was chosen for EuS as target material because it is easy to handle. For Co and Pd, pellets were used. All materials were evaporated from tungsten crucibles at rates between 0.3 and 1.0 Å/s. Thicknesses deposited were checked in situ by a quartz microbalance. Si(111) with native oxide was used as a substrate for all samples. Each sequence started with a Pd buffer layer of a few nanometers followed by the Co/Pd multilayer. Co/EuS multilayers were evaporated on top of the Co/Pd multilayer at the end. All samples terminated with EuS, as it is stable against oxidation. All depositions were carried out at room temperature.

Measurements of the samples were performed *ex situ* in a polar MOKE setup (see [supplementary material](#) Figure S1 for details on the measurement setup). A halogen and a xenon lamp were used as different light sources, providing a range of available photon-energy values between 1.9 eV and 4.7 eV. The magnetic field could be varied between 0 and 2.2 T. Measurements in remanence were carried out by first saturating the sample at 2.2 T and then reducing the external field to 0 T prior to measuring.

^{a)}Electronic mail: alexander.goschew@fu-berlin.de



TABLE I. Overview of samples and magnetic substrates. Numbers in parentheses denote the thickness in Ångström.

| Sample name | Substrate | Structure |
|-------------------------|----------------------------|--------------------------|
| Magnetic substrate (MS) | Si(111) + SiO ₂ | Pd(70)[Co(6)/Pd(20)] × 4 |
| Sample A | MS | [Co(10)/EuS(20)] × 3 |
| Sample B | MS | [Co(15)/EuS(40)] × 2 |
| Sample C | MS | [Co(20)/EuS(40)] × 2 |

Initial work focused on designing a suitable Co/Pd multilayer (“magnetic substrate,” MS) in order to introduce perpendicular magnetic anisotropy (PMA) in the layers deposited on top of the MS. It is known from literature that Co/Pd multilayers exhibit PMA.¹² Prior work on magnetic substrates (with platinum) in our group facilitated the choice of layer thicknesses and number of layer repetitions.^{13,14}

A Pd(70 Å)[Co(6 Å)/Pd(20 Å)] × 4 multilayer turned out to be the optimal MS, with a squareness of 95%. The squareness is defined by $S = \frac{\theta_{K,rem}}{\theta_{K,sat}}$, where $\theta_{K,rem}$ and $\theta_{K,sat}$ are the Kerr rotations at remanence and saturation, respectively. This definition is consistent with the corresponding definition used for magnetic hysteresis loops. Additional Co and Co/Pd overlayers were evaporated thereafter to check how much PMA would still be present for larger Co thicknesses on top. Co/Pd overlayers with 2 nm Co thickness were found to show a squareness of 61% (see Fig. S2). As a last step, the Co/EuS multilayers were added on top of the designed magnetic substrate. Table I gives an overview of the structure of all samples investigated in this work.

Hysteresis loops of the samples A, B, and C were recorded at 2.5 and 4.1 eV and are shown together with the MS hysteresis loop recorded at 2.5 eV in Fig. 1. For better clarity, the loops are shifted by 0.5° each along the y-axis. At 2.5 eV, the samples show a substantial degree of squareness that decreases from sample A (85%) to B (65%) to C (45%) with increasing

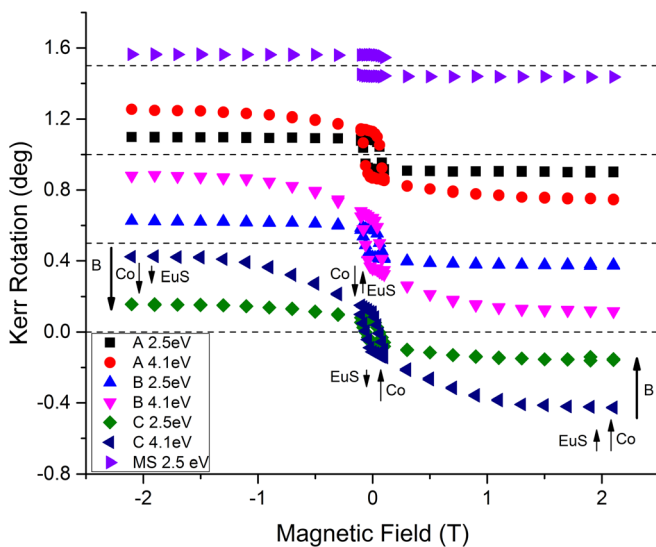


FIG. 1. Polar Kerr hysteresis loops of samples A, B, and C recorded at 2.5 and 4.1 eV and of the MS at 2.5 eV. The Kerr hysteresis loops are consecutively offset by 0.5° each along the vertical axis for clarity. Dashed horizontal lines mark the zero line. The orientation of Co and EuS magnetic moments relative to the applied magnetic field B is exemplarily indicated by arrows for sample C at 4.1 eV.

individual Co layer thickness in the Co/EuS multilayers. The coercive fields are in the range of 100 mT, comparable to the magnetic substrates. Sample A appears to be saturated over the whole scanning range, sample B saturates between 500 and 700 mT, and sample C at around 1 T.

However, despite the anticipated antiferromagnetic coupling between Co and EuS, the hysteresis loops at 2.5 eV do not show any sign of a possible rotation of the EuS magnetic moments. This is due to the small amount of absorption in thin EuS layers for this energy range¹⁵ and the small to negligible contribution of EuS at room temperature. Hysteresis loops recorded at 4.1 eV show slightly different behavior. All samples now saturate only at higher magnetic fields and do not show the same degree of squareness as before. Sample A saturates at around 1.5 T and has around 60% squareness. Samples B and C saturate at 1.3 and 1.5 T with about 46 and 23% squareness, respectively. The absolute Kerr rotation is larger at 4.1 eV compared to 2.5 eV for all samples which is partly due to a larger Kerr rotation of Co at this energy. However, this effect would not lead to a different saturation behavior of the whole sample. The polar Kerr rotation at a specific photon energy is not just proportional to the magnetization but to the joint density of states of the initial and final state of the electronic transition induced by the photon.¹⁶ Therefore, the different shape of the hysteresis loops at higher energies is caused by different electronic contributions. We believe that the measurements at 4.1 eV show the influence of EuS as well as Co due to an increased EuS Kerr signal in the ultraviolet energy range compared to lower energies. This enhanced visibility of EuS at higher energies is due to a known magneto-optic enhancement effect between Co and EuS.¹⁷ Because MOKE is not an element specific method *per se*, it is not easy to directly disentangle the EuS and Co signals at 4.1 eV. The measured Kerr rotations θ_K are given by the following relations:

$$\theta_{K,2.5\text{eV}} = \theta_{K,Co,2.5\text{eV}} + \theta_{K,EuS,2.5\text{eV}} \cong \theta_{K,Co,2.5\text{eV}}, \quad (1)$$

$$\theta_{K,4.1\text{eV}} = \theta_{K,Co,4.1\text{eV}} + \theta_{K,EuS,4.1\text{eV}}, \quad (2)$$

$$\theta_{K,Co,4.1\text{eV}} = \alpha \times \theta_{K,Co,2.5\text{eV}}, \quad (3)$$

where α is the scaling factor between the Co Kerr rotation at 4.1 and 2.5 eV. Equation (2) can be rearranged to get the EuS Kerr rotation at 4.1 eV

$$\theta_{K,EuS,4.1\text{eV}} = \theta_{K,4.1\text{eV}} - \alpha \times \theta_{K,Co,2.5\text{eV}}. \quad (4)$$

As the measurements at 2.5 eV reveal no clear evidence of a EuS contribution, we assume these measurements to show a “pure” Co hysteresis curve. In order to get a suitable factor α , Kerr spectra of all samples were recorded in remanence and at 2.2 T. They are shown in Fig. 2.

In the low-energy range (1.9–2.1 eV), the spectra at remanence and at 2.2 T do not differ significantly for sample A. This is due to the very high degree of PMA for this sample. At energies larger than 2.1 eV, the two spectra start to differ though the difference at 2.5 eV is still small. At higher energies between 4.1 and 4.3 eV, there is a pronounced negative peak in the spectra for all samples recorded at 2.2 T due to a magneto-optic enhancement effect.¹⁷ In remanence, the peak

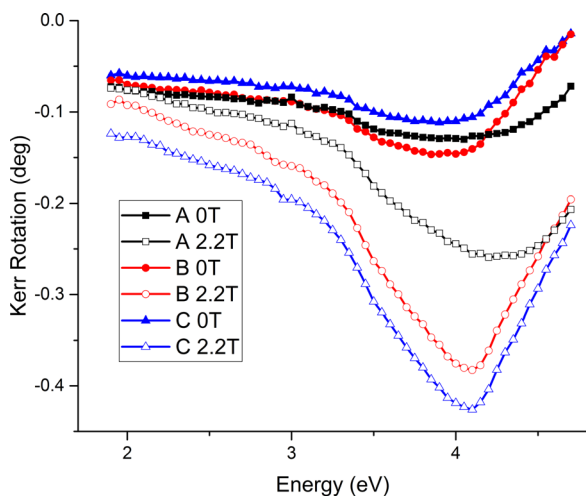


FIG. 2. Polar Kerr spectra of samples A, B, and C recorded at remanence (0T) and at 2.2T.

is less pronounced. The peak positions for samples B and C coincide but differ from sample A, where the peak is also less clear and shows a blue shift.

The magneto-optic enhancement effect at the Co/EuS interface is very sensitive to the local properties of the interface. It is influenced not only by the single Co/EuS interface but also by the number and thickness of the multilayer constituents. In previous work,¹³ it was found that the position of the peak varies mainly with EuS film thickness. For larger thickness, a red shift is observed and for small thicknesses a blue shift. The width of the peak will depend on the quality of the multilayers and interfaces. As has been reported for similar multilayers, the quality of growth decreases with the number of layer repetitions.⁴ It cannot be excluded that sample A, which has the highest number of repetitions, has a slightly worse interface quality as compared to samples B and C (same number of repetitions), resulting in a less pronounced peak.

In the case of samples B and C, the two spectra do not coincide at low energies. This is because both samples show less than 100% PMA which leads to a smaller Kerr signal at remanence as opposed to an applied field. For the spectra measured at 2.2 T, the absolute rotations are increasing from sample A to C due to the increasing of the Co overall thickness. The opposite is true for the spectra recorded at remanence as the degree of PMA decreases from sample A to C.

Assuming an antiferromagnetic exchange coupling to be present between Co and EuS, as previously measured with XMCD in similar systems, we made the following assumptions:

- (i) At remanence, Co and EuS are antiferromagnetically exchange coupled and their magnetic moments are opposite.
- (ii) A magnetic field of 2.2 T is enough to break the exchange coupling between Co and EuS, which will lead to a parallel alignment of their magnetic moments.

In order to account for the difference in the remanence and applied field spectra for samples B and C at low energies, we matched both spectra at 1.9 eV by multiplying the remanence spectra by a suitable factor. This seemed reasonable, given that for sample A the remanence and applied field

spectra do not differ at this energy. After matching the spectra, the average of the remanence and applied field spectra was calculated in order to cancel out the supposed EuS influence in accordance with assumption (ii). The result was three spectra showing the contribution of Co only. With this method, it was possible to calculate α for each sample individually. The factor α was then used to multiply the recorded hysteresis loops of samples A, B, and C at 2.5 eV according to Equation (3) and subtract the multiplied loops from the ones recorded at 4.1 eV, leaving only the EuS contribution to the polar Kerr rotation at 4.1 eV, in agreement with Equation (4). The results are shown in Fig. 3. For better clarity, samples A and B have been shifted along the y-axis by 0.4° and 0.2°, respectively.

Arrows indicate the direction of magneto-optic signal reversal for each hysteresis loop. In the case of sample A, the polar Kerr signal is saturated above 1.3 T reaching a value between -0.04 and -0.05 (0.36° – 0.35° in Fig. 3). Decreasing the magnetic field to zero increases the EuS signal (zero crossing at around 0.5 T) to 0.05° (0.45° in Fig. 3) at remanence. The signal stays constant until approximately -100 mT, where it flips abruptly to -0.05° (0.35° in Fig. 3) in very good agreement with the observed flipping of the entire Co/EuS signal [Fig. 1, samples A-C] after which it increases with increasing magnetic field (zero crossing at -0.5 T) until it saturates between 0.04° and 0.05° (0.44° – 0.45° in Fig. 3). The hysteresis loop is symmetric and shows clear evidence of antiferromagnetic coupling. Because the PMA of sample A is very high, the absolute EuS signal at remanence and at maximum field is the same.

The opposite sign of the polar Kerr rotation at high magnetic field and at remanence points to a rotation of the EuS magnetic moment from antiparallel alignment at remanence to fully parallel alignment with the Co magnetic moment at a magnetic field of 1.3 T and beyond. For samples B and C, the hysteresis loops have a similar shape. The sign of the Kerr rotation at remanence (positive) and under maximum applied field (negative) also gives evidence of an antiferromagnetic alignment between Co and EuS magnetic moments. The absolute values of the polar Kerr rotation at

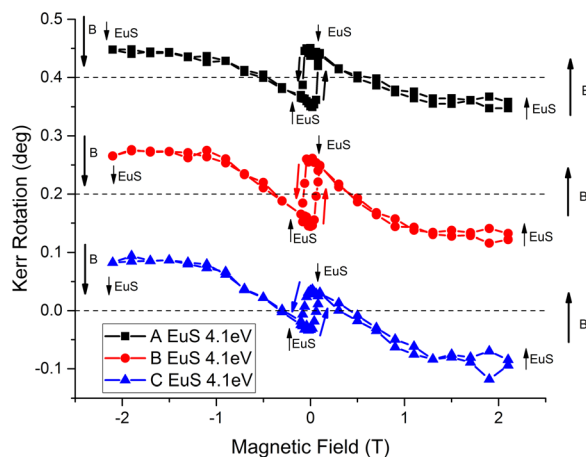


FIG. 3. EuS polar-Kerr hysteresis loops derived at 4.1 eV for samples A, B, and C. Each curve is consecutively offset by 0.2° along the vertical axis for clarity. Dashed horizontal lines mark the zero line. The orientation of the EuS magnetic moments relative to the applied magnetic field B is indicated by arrows.

remanence and in maximum applied field are not the same for samples B and C because for these samples the degree of PMA is less than 100%, meaning that at remanence part of the EuS magnetic moment is no longer oriented out of plane and does no longer contribute to the polar Kerr rotation. In maximum magnetic field, however, all the magnetic moments have been rotated out of plane and contribute to an overall larger signal compared to remanence. The absolute maximum value of the polar Kerr rotation of EuS at 4.1 eV is increasing from sample A (0.05°) to sample C (0.08°) which could be due to either a stronger coupling due to increasing Co thickness in the Co/EuS bilayers (in case of an interface coupling effect) or increasing the EuS thickness in the bilayers in the samples (double for samples B and C compared to A) if the Co-induced polarization of the EuS layers extends significantly into the interior. As this has not been investigated in detail yet, it is hard to give a conclusive answer.

We will now shortly discuss our results and possible errors that could have been made. In order to extract the EuS signal at 4.1 eV, a couple of assumptions were made. One of them, the antiferromagnetic exchange coupling between Co and EuS at room temperature, is motivated by XMCD on similar Co/EuS multilayers, where the antiferromagnetic coupling was found to be present at low temperatures and at room temperature.⁴ The Eu XMCD signal at room temperature was significantly reduced compared to low temperature, yet antiferromagnetic coupling was still found. Because the exchange coupling strength is expected to decrease, the assumptions (i) and (ii) stated above seem reasonable.

As there was no clear evidence of any antiferromagnetic coupling in the hysteresis loops recorded at 2.5 eV, it was assumed that the EuS signal is negligible and that the recorded hysteresis loops at 2.5 eV show predominantly the Co Kerr rotation. However, a closer look at the recorded spectra in remanence and under applied field reveals that, although the difference between the two spectra is negligible for energies from 1.9 to 2.1 eV, there is a small difference at 2.5 eV. The deviation of the “pure” Co signal at 2.5 eV (calculated by averaging the spectra) from the one in the Kerr hysteresis loop at 2.5 eV amounts from about 7% (sample C) to about 15% (sample A). For this reason, the calculated factors from the “pure” Co spectrum linking 2.5 and 4.1 eV, which were used to calculate the EuS signal at 4.1 eV, were altered in order to check how reliable the calculated signal was. The calculated α values were 2.1 (1.8–2.4) for sample A, 2.5 (2.0–4.0) for sample B, and 2.2 (1.8–3.5) for sample C (values given in brackets are the tested range for which similar hysteresis loops to the ones shown in Fig. 3 were obtained). The factors tested exceed the uncertainty range of up to 15% error in the Co 2.5 eV hysteresis loops significantly and make the calculated EuS Kerr rotation at 4.1 eV and the general conclusion of the presence of antiferromagnetic exchange coupling quite robust.

Another source of error could be the misinterpretation of the additional signal in the hysteresis loops recorded at 4.1 eV as ferromagnetic instead of paramagnetic EuS signal. A paramagnetic signal would still be optically enhanced by the same enhancement effect mentioned above. For this reason, we assumed only paramagnetic response from EuS in

the 4.1 eV hysteresis loops and chose the factors to cancel out the Co signal in such a way that the Kerr rotation disappears for zero magnetic field. The factors for which this happened were 1.5 (A), 1.77 (B), and 1.66 (C). The so calculated hysteresis loops showing EuS contribution at 4.1 eV were averaged (decreasing and increasing magnetic field summed). Fitting these curves with a Brillouin function led to J values between 530 and 760. Values this high can only occur when one treats nanoparticles as magnetic entities in superparamagnetism, which is not the case here, as the quality of the growth of such multilayers has already been checked.⁴ In fact, paramagnetic EuS with $7\mu_B$ and $T_C = 16.5$ K would render a straight line and not saturate for the magnetic field range applied in our experiments. In contrast, the hysteresis loops obtained for the supposed paramagnetic EuS signal show saturation above 1.5 T (see Figure S3).

In light of the very high values for J found from the Brillouin-fits, we doubt that the additional signal at 4.1 eV is due to bulk paramagnetic EuS. It is at least due to EuS with considerably higher T_C than the bulk value of 16.5 K and given the XMCD results showing ferromagnetism in EuS in similar multilayers at room temperature, we attribute this signal-change at 4.1 eV to the same antiferromagnetic exchange mechanism in Co/EuS structures and thus to ferromagnetism in EuS.

In conclusion, polar MOKE measurements were carried out on three different EuS/Co multilayers deposited on top of Co/Pd “magnetic substrates” which introduced perpendicular magnetic anisotropy in the Co/EuS multilayers. All samples show a high degree of perpendicular magnetic anisotropy. Polar Kerr hysteresis loops and polar Kerr spectra were recorded at room temperature, where bulk EuS is paramagnetic. The contribution of EuS to the Kerr rotation is small to negligible at low energies but clearly visible at higher energies due to increased absorption and a magneto-optic enhancement effect between Co and EuS. Within a simple model, the polar Kerr hysteresis loops of EuS were extracted at 4.1 eV showing antiferromagnetic coupling to Co. A paramagnetic signal from bulk EuS can be excluded as a reason for the hysteresis loops’ changes at higher energies. With this analysis, we have proven that magneto-optic Kerr effect spectroscopy can be used here as a quasi-element-specific method.

See [supplementary material](#) for details about the measurement setup, the magnetic substrates, and Brillouin function fits of the data.

¹S. v. Houten, *Phys. Lett.* **2**(5), 215 (1962).

²S. Demokritov, U. Rucker, and P. Grünberg, *J. Magn. Magn. Mater.* **163**, 21 (1996).

³P. Fumagalli, J. Schirmeisen, and R. J. Gambino, *Phys. Rev. B* **57**, 14294 (1998).

⁴S. D. Pappas, P. Pouloupoulos, B. Lewitz, A. Straub, A. Goschew, V. Kapaklis, F. Wilhelm, A. Rogalev, and P. Fumagalli, *Sci. Rep.* **3**, 1333 (2013).

⁵P. Pouloupoulos, A. Goschew, V. Kapaklis, M. Wolff, A. Delimitis, F. Wilhelm, A. Rogalev, S. D. Pappas, A. Straub, and P. Fumagalli, *Appl. Phys. Lett.* **104**, 112411 (2014).

⁶M. S. S. Brooks, L. Nordström, and B. Johansson, *J. Appl. Phys.* **69**, 5683–5684 (1991).

⁷B. Scholz, R. A. Brand, and W. Keune, *Hyperfine Interact.* **68**, 409–412 (1992).

- ⁸U. Rücker, S. Demokritov, R. R. Arons, and P. Grünberg, *J. Magn. Magn. Mater.* **156**, 269–270 (1996).
- ⁹J. Tang, C. E. O'Connor, and L. Feng, *J. Alloys Compd.* **275–277**, 606–610 (1998).
- ¹⁰M. Szot, L. Kowalczyk, K. Gas, V. Domukhovski, W. Knoff, V. V. Volobuev, A. Y. Sipatkov, A. G. Fedorov, and T. Story, *Acta Phys. Pol. A* **114**(5), 1397–1402 (2008).
- ¹¹R. J. Gambino and P. Fumagalli, *IEEE Trans. Magn.* **30**, 4461 (1994).
- ¹²G. G. An, J. B. Lee, S. M. Yang, W. S. Chung, K. S. Yoon, and J. P. Hong, *AIP Adv.* **5**, 027137 (2015).
- ¹³C. Müller, H. Lippitz, J. J. Paggel, and P. Fumagalli, *J. Appl. Phys.* **95**(11), 7172 (2004).
- ¹⁴C. Müller, H. Lippitz, J. J. Paggel, and P. Fumagalli, *J. Appl. Phys.* **99**, 073904 (2006).
- ¹⁵P. Pouloupoulos, B. Lewitz, A. Straub, S. D. Pappas, S. A. Droulias, S. Baskoutas, and P. Fumagalli, *Appl. Phys. Lett.* **100**, 211910 (2012).
- ¹⁶J. L. Erskine and A. Stern, *Phys. Rev. Lett.* **30**(26), 1329 (1973).
- ¹⁷P. Fumagalli, C. Spaeth, U. Rüdiger, and R. J. Gambino, *IEEE Trans. Magn.* **31**(6), 3319 (1995).